

Physics of Radioactive Beams¹
Chapter 9
Tests of Fundamental Interactions

Carlos A. Bertulani, Texas A&M University-Commerce, TX 75429, USA

¹These notes consist of a series of lectures presented by the author at the Gesellschaft für Schwerionenforschung, Darmstadt, Germany in the Spring of 1994. GSI-Report 1994-11. This material was latter extended and published in the book “Physics of Radioactive Beams”, C.A. Bertulani, M. Hussein and G. Muenzenberg, Nova Science, Hauppauge, NY, 2002, ISBN: 1-59033-141-9

0.1 Introduction

The parity nonconserving (PNC) nucleon interaction in nuclei caused by the PNC Weak interaction, and PNC effects in neutron-nucleus reactions are subject of interest for both experimentalists and theorists [1, 2, 3, 4, 5, 6, 7, 8, 9]. The overall scale of the observable PNC effects is found to be in reasonable agreement with estimates in existing theory of the weak interactions [1] based on the Standard Model. Complete understanding of PNC forces in nuclear domain, which requires reliable QCD-based models of hadrons is far from being reached. This motivates extensive studies of the strengths of the PNC forces.

The PNC effects have been probed in normal nuclei. Physics of exotic nuclei studied with unstable nuclear beams [10, 11, 12, 13, 14, 15, 16, 17, 18, 20, 21, 22, 23] appears to be one of the most promising modern nuclear areas. Due to their specific structure, exotic nuclei, e.g., halo nuclei can offer new possibilities to probe those aspects of nuclear interactions which are not accessible with normal nuclei. It is therefore interesting to examine possibilities of using exotic nuclei to investigate the effects of violation of fundamental symmetries, i.e., spatial parity and time reversal.

Some aspects of the Weak interactions in exotic nuclei have been discussed in literature [17, 18] in relation to the beta decay and to possibilities to study the parameters of the Cabibbo-Kobayashi-Masawa matrix.

The aim of the next sections is to present a simple evaluation of the magnitude of the PNC effects in halo nuclei, following Hussein et al. [19]. We confine ourselves to the case of nucleus ^{11}Be , the most well studied, both experimentally and theoretically [10, 11, 12, 15, 16]. One finds that the ground state, the $2s_{1/2}$ halo configuration, acquires admixture of the closest in energy halo state of opposite parity, $1p_{1/2}$. This effect originates from the weak interaction of the external halo neutron with the core nucleons in the nuclear interior. As a result, the neutron halo cloud surrounding the nucleus acquires the wrong parity admixtures that may be tested in experiments which can probe the halo wave functions in the exterior.

The magnitude of the admixture is found to be $\sim 10^{-6} \times g_n^W$ that is an order of magnitude bigger than the PNC effects in normal spherical nuclei. What is important to notice is that the enhanced effect discussed here is proportional to the *neutron weak constant* g_n^W only. The value of this constant remains to be one of the most questionable points in modern theory of parity violation in nuclear forces [5]. The enhanced PNC mixing in halo found here can be therefore useful in studies of the neutron weak constant. Another interesting question related to the structure of the PNC force in nucleus, namely, the strength of the isovector P-odd potential that has been discussed in Refs. [6, 7].

0.2 Weak nucleon-nucleon interaction and parity violating effects. Potential approximation

We start with writing the nuclear Hamiltonian H in the form

$$H = H_S^0 + V_S^{res} + W^{PNC}, \quad (1)$$

where the first term $H_S^0 = \sum_a (\mathbf{p}_a^2/2m + U_S(\mathbf{r}_a))$ is the single particle Hamiltonian of the nucleons including the single-particle piece U_S of the strong interaction, V_S^{res} is the residual two-body strong interaction. The last term, W^{PNC} is the PNC part of the Weak interaction that is the source of the PNC effects.

The magnitude of the PNC effects is sensitive to both the weak PNC interaction matrix elements between the states of opposite parity and to the nuclear structure effects given by the strong part of the Hamiltonian 1. The latter one is invariant under spatial coordinate reflections, and if there is no weak interaction term W^{PNC} in 1, and as such parity is preserved, the eigenstates $|\Psi_s\rangle$ of the strong Hamiltonian $H_S^0 + V_S^{res}$ with energies E_s can be labeled by the parity quantum number (positive or negative), $|\Psi_s^+\rangle$, $|\Psi_s^-\rangle$. Due to presence of PNC weak interaction W^{PNC} in the nuclear Hamiltonian 1, a state of definite parity, say, $|\Psi_s^+\rangle$, acquires very small admixtures of wrong parity configurations. This can be accounted for by using the first order of perturbation theory with respect to W^{PNC} (see Eq. ??):

$$|\Psi_s^+\rangle' = |\Psi_s^+\rangle + \sum_{s1} \frac{\langle \Psi_{s1}^- | W^{PNC} | \Psi_s^+ \rangle}{E_s - E_{s1}} |\Psi_{s1}^-\rangle. \quad (2)$$

Here, prime denotes the corrected wave function that accounts for the PNC interaction and sum goes over available states of opposite parity, $|\Psi_{s1}^-\rangle$. The magnitude of measurable PNC effects is normally proportional to the coefficients f^{PNC} [2] that determine the dominating admixtures of the wrong parity states

$$f = \frac{\langle \Psi_{s1}^- | W^{PNC} | \Psi_s^+ \rangle}{\Delta E}. \quad (3)$$

The natural scale of the PNC effects in nuclei under usual conditions is [1],[2]

$$|f| \simeq 10^{-7} \quad (4)$$

that is roughly the ratio of the strength of the Weak PNC forces (matrix element in the numerator of 3) and the strength of the strong interaction (energy denominator in 3). In highly selective experiments, the PNC effects can be enhanced considerably as compared to estimate 4, due to specific properties of a specially chosen nuclear system or process. To reach high sensitivity to the wrong parity admixtures, one usually seeks possibilities to

have the denominator ΔE in 3 minimal while keeping the PNC matrix element at maximum and to improve selectivity of measurable effect. This is typical for any tests of fundamental symmetries.

Supplement A

0.3 Microscopic PNC interaction

The most widely used version of the microscopic PNC interaction is the DDH Hamiltonian W_{DDH}^{PNC} [1], where the PNC forces are mediated by mesons. Its form stems from the analysis of interactions between intranucleon quarks via exchange of heavy bosons of Standard Model. The nonrelativistic P-odd weak interaction between nucleons approximated by the one-meson exchange can be written in the form [2, 1]

$$\begin{aligned}
 W_{DDH}^{PNC} = & i \frac{h_\pi^{(1)} g_\pi}{4\sqrt{2}m} (\tau_1 \times \tau_2)^{(3)} (\sigma_1 + \sigma_2) \cdot [\mathbf{p}_1 - \mathbf{p}_2, \mathcal{F}_\pi] - \\
 & - \frac{g_\rho h_\rho^0}{2m} (\tau_1 \cdot \tau_2) (\sigma_1 - \sigma_2) \cdot \{\mathbf{p}_1 - \mathbf{p}_2, \mathcal{F}_\rho\} - \\
 & - \frac{g_\rho h_\rho^0}{2m} i(1 + \mu) (\tau_1 \cdot \tau_2) (\sigma_1 \times \sigma_2) \cdot [\mathbf{p}_1 - \mathbf{p}_2, \mathcal{F}_\rho] + W', \quad (5)
 \end{aligned}$$

where the standard notations $F_{\pi(\rho)} = e^{-m_{\pi(\rho)}|\mathbf{r}_1 - \mathbf{r}_2|} / (4\pi|\mathbf{r}_1 - \mathbf{r}_2|)$ are used and $[\cdot, \cdot]$ and $\{\cdot, \cdot\}$ denote the commutator and anticommutator, respectively. The subscripts 1 and 2 label the interacting nucleons, the superscript (3) denotes the third isospin projection. Here, m , m_π and m_ρ are the masses of the nucleon, π - and ρ -meson, respectively; σ (τ) stand for the spin (isospin) Pauli matrices, $\mu = 3.7$ is the isovector part of the anomalous magnetic moment of nucleon. W' denotes contributions from heavier mesons, which are less important. The values of the corresponding weak and strong coupling constants $h_\pi^{(1)}$, g_π , g_ρ , and h_ρ^0 can be found in [1, 2].

0.4 Effects of the nuclear environment

In nuclear environment, a nucleon experiences the combined action of the PNC forces 5 from other nucleons. It is known, see, e.g., [2], that the most of P-odd effects caused by the weak interaction W_{DDH}^{PNC} , Eq. 5 in Eq. 1, can be successfully modeled by introducing the effective one-body P-odd interaction, or the “weak potential”, W_{sp} , acting on the nucleon 1 as a single-particle operator which arises from averaging W^{PNC} over the states of other nucleons $W_{sp} \equiv \langle W^{PNC} \rangle$. Within this approximation, the Hamiltonian of the weak interaction in a

nucleus takes particularly simple form of a sum of the proton W_{sp}^p and neutron W_{sp}^n symmetry violating potentials

$$W_{sp} = W_{sp}^p + W_{sp}^n = g_p^W \frac{G}{2\sqrt{2}m} \{(\sigma_p \cdot \mathbf{p}_p), \rho\} + g_n^W \frac{G}{2\sqrt{2}m} \{(\sigma_n \cdot \mathbf{p}_n), \rho\}, \quad (6)$$

where $G = 10^{-5}m^{-2}$ is the Fermi constant, $\mathbf{p}_{p(n)}$ and $\sigma_{p(n)}$ refer to the proton (neutron) momentum and doubled spin respectively. The coherent contribution from all the occupied nucleon orbitals composing the core yields the nuclear density $\rho = \sum_{occ} |\psi_{occ}|^2$ in the expression 6. The dimensionless constants g_p^W and g_n^W of order of unity, for the proton and neutron potentials, are related to the parameters of the DDH Hamiltonian and depend on nuclear charge and neutron number. The single-particle approximation 6 for the PNC weak interaction 5 turns out to be very accurate [2]. It works satisfactorily even in the case of compound nuclear states [4, 26, 27, 28] where 6 gives the dominating contribution [26, 27] despite the fact that the wave functions are of essentially many-body nature.

0.5 Proton and neutron weak potential strengths

The knowledge about the proton and neutron constants g_p^W and g_n^W accumulated to date can be summarized as follows:

$$g_p^W = 4.5 \pm 2, \quad g_n^W = 1 \pm 1.5. \quad (7)$$

These widely used values [2, 5, 25, 26] correspond to the best values [1] of the microscopic parameters in the DDH Hamiltonian, Eq. 5, and they are found in reasonable agreement with the bulk experimental data on parity violation, including the compound nuclear experiments [3] and anapole moment measurements [32]. The above relatively small absolute value of the neutron constant that follows from DDH analysis, results basically from cancellation between π - and ρ -meson contributions to g_n^W , while both mesons contribute coherently to the proton constant g_p^W , see, e.g., [5]. Due to this difference between the absolute values of the proton and neutron constants, the proton constant tends to dominate most measurable PNC effects [24, 25, 29, 30], especially when both g_p^W and g_n^W can contribute. In some cases (such as odd proton nuclei), the contribution from the neutron constant, g_n^W , is suppressed irrespectively of its strength [2, 6]. In this sense, one usually measures the value of g_p^W , and it is difficult to probe g_n^W unless special suppression of the proton contribution occurs, and/or contribution of g_n^W is highlighted. By contrast, the case we consider in this work is sensitive to the value of the neutron constant only.

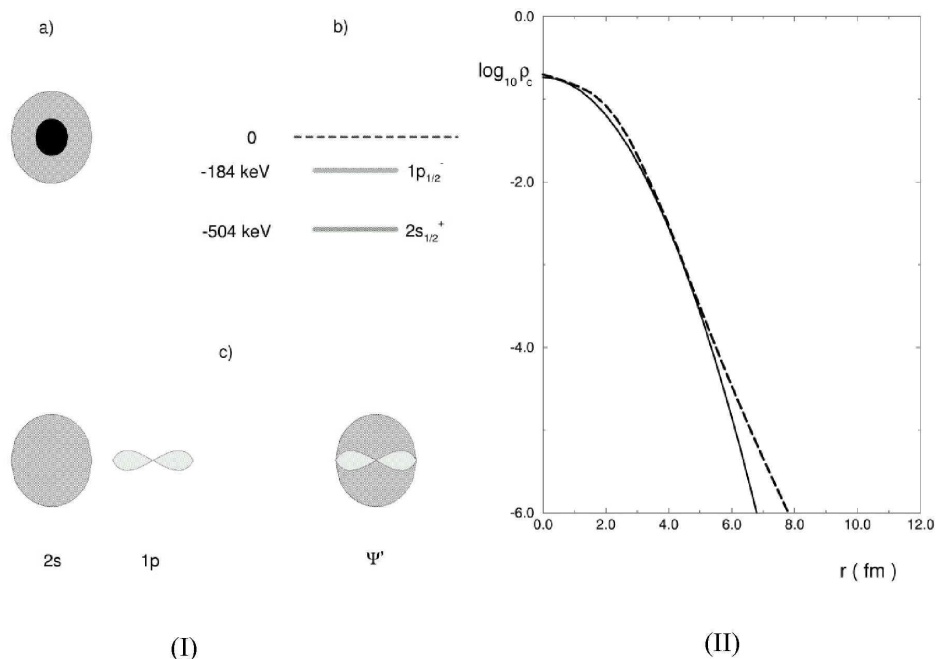


Figure 1: (I) a) Schematic plot of matter distribution in halo nuclei. The dark region corresponds to the nuclear core, the grey region shows the halo neutron cloud. b) The spectrum of the bound states ^{11}Be . c) Illustration of the single-particle PNC mixing in the ground state of ^{11}Be . (II) The core density distribution (logarithmic scale). The dashed line corresponds to Ref. [12], the solid line gives parametrization 15.

0.6 Halo structure effects on the PNC mixing

The basic specific properties of the halo nuclei are determined by the fact of existence of loosely bound nucleon in addition to the core composed by the rest of the nucleons [13] (we will be interested here in the most well studied case of neutron halo). The matter distribution is shown schematically in Fig. 1(I-a).

In one-body halo nuclei like ^{11}Be , the ground state is particularly simple: it can be represented as direct product of the single-particle wave function of the external neutron, ψ_{halo} , and the wave function of the core. The residual interaction V_S^{res} in Eq. 1 can be neglected as the many-body effects related to the core excitations are generically weak in such nuclei [34]. The problem with the Hamiltonian 1 is reduced to a single-particle problem for the external nucleon. The PNC potential matrix element between the ground state of halo nucleus and a state with opposite parity is

$$\langle \psi_{halo}^+ | W^{PNC} | \psi_{halo}^- \rangle = g_n^W \frac{G}{2\sqrt{2}m} \langle \psi_{halo}^+ | \{ (\sigma_n \cdot \mathbf{p}_n), \rho_c \} | \psi_{halo}^- \rangle, \quad (8)$$

where $\rho_c(r)$ is the core density. Due to relatively heavy core for $A \simeq 10$, the difference between the center of mass coordinate and the center of core coordinate can also be neglected.

The effective potential that binds the external neutron is rather shallow yielding a small single-neutron separation energy, and one can expect small energy spacing between the opposite parity states. The PNC effects, Eqs. 3 and 2, can therefore be considerably magnified. The spectrum of ^{11}Be is shown in Fig. 1(I-b). To evaluate the PNC mixing f^{HALO} in the ground state of this nucleus, it is enough to know the single-particle matrix element between the ground state 2s and the nearest opposite parity state 1p, and use their energy separation that is known experimentally.

The second effect of halo is that the value of the matrix element of the operator 6 between the halo states can be dramatically reduced as compared to its value in the case of “normal” nuclear states. The single-particle weak PNC potential 6 in Eq. 8 originates from the DDH Hamiltonian, Eq. 5, which is two-body operator, this fact is hidden in the nucleon density of the core $\rho_c(r)$. The external neutron spends most of its time away from the core region where only it can experience the PNC potential created by the rest of nucleons. Indeed, the dominant contribution to the matrix element of 6 between the halo states in 8 must come from the regions where the three functions can overlap coherently: $\psi_{halo}^+(r)$, $\psi_{halo}^-(r)$ and the core density $\rho_{core}(r)$. The latter one is essentially restricted by the region of nuclear interior, $r < r_c$ thus reducing the effective volume of required interference region to $\frac{4}{3}\pi r_c^3$. Normalization condition implies that the extended wave function of the bound state halo $\psi_{halo}^\pm(r)$ must be considerably reduced in the volume of coherent overlap $\frac{4}{3}\pi r_c^3$. By contrast, in “normal” nuclei the radii of localization of the wave functions with opposite parity that can be mixed by the weak interaction coincide generically with the core radius r_c . The resulting suppression for the PNC halo matrix element $\langle \psi_{halo}^-(r) | W_{sp} | \psi_{halo}^+(r) \rangle$ with respect to the matrix element for the normal nuclei can be extracted from the following simple estimate

$$\frac{\langle \psi_{halo}^- | W_{sp} | \psi_{halo}^+ \rangle}{\langle \psi_{normal}^- | W_{sp} | \psi_{normal}^+ \rangle} \sim \left(\frac{r_c}{r_{halo}} \right)^3 \sim \left(\frac{2\text{fm}}{6\text{fm}} \right)^3 \sim \frac{1}{25} \cdots \frac{1}{30} \quad (9)$$

where the mean square radii of halos from Ref. [12] was used. This suppression factor can cancel out the effect of the small energy separation (the denominator in Eq. 3) and to suppress the PNC effects. This simple estimate does not account for the structure of the halo wave functions which can be quite substantial and may even lead to further suppression in the PNC mixing. In the following, we present a detailed analysis of the related effects. The crude estimate 9 turns out rather pessimistic.

0.7 Halo model and evaluation of the PNC mixing in the ground state of ^{11}Be

The form of the single-particle wave functions of halo states can be deduced from their basic properties [16] and their quantum numbers [12]. The results of the Hartree-Fock calculations which reproduce the main halo properties (e.g., mean square radii) are also available [12]. One can use the following ansatz for the model wave function of the $2s$ halo state:

$$\psi_{2s} = R_{2s}(r)\Omega_{j=1/2,m}^{l=0}, \quad R_{2s}(r) = C_0(1 - (r/a)^2)\exp(-r/r_0). \quad (10)$$

Here, $R_{2s}(r)$ is the radial part of the halo wave function and $\Omega_{j=1/2,m}^{l=0}$ is the spherical spinor. As we can neglect the center of mass effect for the heavy ($A = 10$) core, the halo neutron coordinate r in $R_{2s}(r) = \chi_{2s}(r)/r$ is reckoned from the center of nucleus. The constant C_0 is determined from the normalization condition, $\int_0^\infty dr [\chi_{2s}(r)]^2 = 1$ (the radial wave functions are chosen to be real). One has

$$C_0 = \frac{2^{3/2}a^2}{r_0^{3/2}\sqrt{45r_0^4 + 2a^4 - 12a^2r_0^2}}. \quad (11)$$

The parameters r_0 and the a are the corresponding lengths to fit the density distributions obtained in Ref. [12] and the mean square radius. The value of a is practically fixed to be $a = 2\text{fm}$ what corresponds to the position of the node. The node position have been restored from the analysis of the scattering process [16].

For the wave function $\psi_{1p} = R_{1p}(r)\Omega_{j=1/2,m}^{l=1}$ of the excited state $1p$, the following simplest form of the radial wave function turns out to be adequate

$$R_{1p}(r) = C_1 r \exp(-r/r_1), \quad (12)$$

where C_1 is the normalization constant $C_1 = \frac{2}{\sqrt{3}}r_1^{-5/2}$ and the only tunable parameter r_1 is related to the $1p$ halo radius. The mean square root radii for the halo wave states, Eqs. 10 and 12, are given by

$$\sqrt{\langle r_{2s}^2 \rangle} = r_0 \left(\frac{6(45r_0^4 + 2a^4 - 12a^2r_0^2)}{105r_0^4 + a^4 - 15a^2r_0^2} \right)^{1/2}, \quad \sqrt{\langle r_{1p}^2 \rangle} = \left(\frac{15}{2} \right)^{1/2} r_1. \quad (13)$$

The matrix element of the weak interaction 6 and 8 between the ground state and the first excited state reads

$$\langle 2s | W_{sp} | 1p \rangle = ig_n^W \frac{G}{\sqrt{2}m} \int_0^\infty dr \chi_{2s}(r) \left(\rho_c(r) \frac{d}{dr} + \frac{\rho_c(r)}{r} + \frac{1}{2} \frac{d\rho_c(r)}{dr} \right) \chi_{1p}(r). \quad (14)$$

The core nucleon density $\rho_c(r)$ has been tuned to reproduce the data obtained from Ref. [12]. Their results are well reproduced by the Gaussian-shaped ansatz $\rho_c(r)$,

$$\rho_c(r) = \rho_0 e^{-(r/R_c)^2} \quad (15)$$

with the values of the parameters $\rho_0 = 0.2\text{fm}^{-3}$ and $R_c = 2\text{fm}$, as shown on Fig. 1(II).

Using the model wave functions 10 and 10 and the core density 15, the required integrals can be done analytically, and one arrives at the result

$$\langle 2s|W|1p\rangle = ig_n^W \frac{G}{\sqrt{2}m} \mathcal{R} \quad (16)$$

where

$$\begin{aligned} \mathcal{R} = & \rho_0 R_c^3 C_0 C_1 \left\{ 3I_2(y) - \left[3 \left(\frac{R_c}{a} \right)^2 + 1 \right] I_4(y) + \right. \\ & \left. + \left(\frac{R_c}{a} \right)^2 I_6(y) - \frac{R_c}{r_1} \left[I_3(y) - \left(\frac{R_c}{a} \right)^2 I_5(y) \right] \right\} \end{aligned} \quad (17)$$

where $y = R_c(r_0 + r_1)/r_0 r_1$ and the functions I_n are given by

$$I_n(y) = \int_0^\infty dx \quad x^n e^{-x^2 - yx} = (-1)^n \frac{\sqrt{\pi}}{2} \frac{d^n}{dy^n} \left[e^{y^2/4} \text{erfc}(y/2) \right],$$

where $\text{erfc}(y)$ is the error function

$$\text{erfc}(y) = 1 - \frac{2}{\sqrt{\pi}} \int_0^y dt \quad \exp(-t^2/2).$$

To obtain the results for the PNC weak interaction matrix element, one can use the parameters r_0 and r_1 in the halo wave functions to fit the radial densities of the halos obtained by H. Sagawa [12].

The results for the best parameters are shown in Figs. 2(a) and 2(b) for the $2s$ and the $1p$ halos, respectively. One sees that the agreement for the densities is good. Below, the values

$$r_0(\text{best value}) = 1.45\text{fm}, \quad r_1(\text{best value}) = 1.80\text{fm}, \quad (18)$$

are used to calculate the matrix elements in Eqs. (14, 16 and 17). The radial wave functions χ are given in Fig. 3(a). To check robustness of the results with respect to variations in the halo structure details, deviations of the both r_0 and r_1 from 18 were used. The values of the

0.7. HALO MODEL AND EVALUATION OF THE PNC MIXING IN THE GROUND STATE OF ^{11}Be

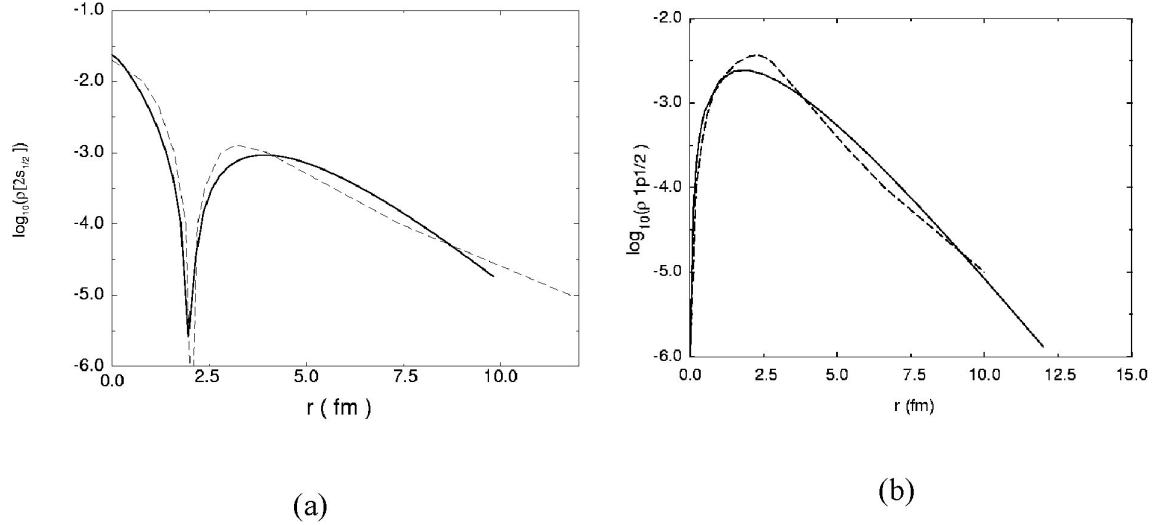


Figure 2: (a) The halo density in the ground state, $\rho_{2s1/2}(r) = (R_{2s1/2}(r))^2 / 4\pi$. The dashed line corresponds to the Hartree-Fock calculations of ref. [12], the solid line gives parametrization 10). (b) The halo density in the first excited state, $\rho_{1p1/2}(r) = \frac{1}{4\pi} (R_{1p1/2}(r))^2$. The dashed line corresponds to the Hartree-Fock calculations of Ref. [12], the solid line gives parametrization 12 and 18.

halo radii given by 13, $\sqrt{\langle r_{2s}^2 \rangle} = 5.9\text{fm}$ and $\sqrt{\langle r_{1p}^2 \rangle} = 4.9\text{fm}$ are close to the values of ref. [12] 6.5fm and 5.9fm which agree with experimental matter radii.

Substituting the values 18 into the expressions for the matrix elements one obtains the following value of the matrix element $\langle 2s | W_{sp} | 1p \rangle_{HALO}$

$$\begin{aligned} \langle 1p | W_{sp} | 2s \rangle_{HALO} &= -i 0.2 g_n^W \text{ eV}, \\ &= -i 0.2 \text{ eV} \quad (\text{for } g_n^W \simeq 1). \end{aligned} \quad (19)$$

It is seen that this value is only few times smaller than the standard value of the matrix element of the weak potential between the opposite parity states in spherical nuclei (see e.g., Ref. [2]), that is typically about one eV . This results from the wave function structure and comes basically from the facts that the $2s$ wave function crosses zero line near the core surface while the $1p$ radial wave function does not have nodes. Thus the functions χ_{1p} and $d\chi_{2s}/dr$ look similar and are folded constructively with $\rho_c(r)$ in the region of interaction (nuclear interior), see Fig. 3(b).

The matrix element of W_{sp} between the “normal” nuclear states can be evaluated for example, in the oscillator model. Taking the typical matrix element between the states $2s$

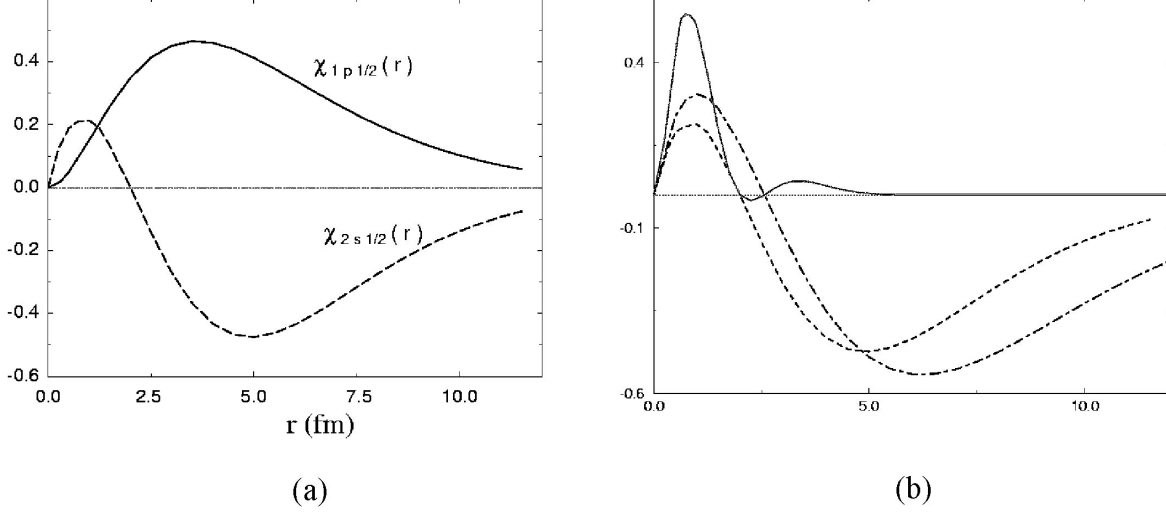


Figure 3: (a) Plot of the radial wave functions of the states $|2s1/2\rangle$ and $|1p1/2\rangle$, $\chi_{2s1/2}(r) = rR_{2s1/2}(r)$ and $\chi_{1p1/2}(r) = rR_{1p1/2}(r)$. (b) Plot of the functions contributing to the weak PNC matrix element. The function $s(r) = \frac{d}{dr}\chi_{1p1/2}(r) + \frac{\chi_{1p1/2}(r)}{r} + \frac{d\rho_c/dr}{2\rho_c}\chi_{1p1/2}(r)$ (dot-dashed line) depends on r in the way similar to $\chi_{2s1/2}(r)$ (dashed line). The combination $\chi_{2s1/2}(r)\rho_c s(r)$ that enters the PNC matrix element in Eq.(14) is shown by the solid line. It contributes coherently to $\langle 2s|W_{sp}|1p\rangle$.

and $1p$ and using the same formula 14, one has

$$\langle 1p|W_{sp}|2s\rangle_{osc} = -ig_n^W G\rho_0 \left(\frac{\omega}{2m}\right)^{1/2} \quad (20)$$

where $\omega \simeq 40A^{-1/3}\text{MeV}$ is the oscillator frequency [33] with A the nuclear mass number. We used here the constant value of the core nucleon density, $\rho_0 \simeq 0.138\text{fm}^{-3}$. This is a good approximation in the case of normal nuclei [26].

Recalling the energy difference between the ground state and the first excited state $1p$ that is known experimentally,

$$|\Delta E_{HALO}| = E_{p1/2} - E_{s1/2} = 0.32\text{MeV} \quad (21)$$

we obtain, using Eq. 19, the coefficient of mixing the opposite parity state ($1p$) to the halo ground state $2s$:

$$\begin{aligned} |f_{sp}^{HALO}| &= \frac{|\langle 1p|W_{sp}|2s\rangle|}{|\Delta E_{HALO}|} \simeq \frac{0.2eVg_n^W}{0.32\text{MeV}} \\ &\simeq 0.6 \times 10^{-6}g_n^W \simeq 0.6 \times 10^{-6} \quad (\text{for } g_n^W \simeq 1). \end{aligned} \quad (22)$$

0.7. HALO MODEL AND EVALUATION OF THE PNC MIXING IN THE GROUND STATE OF ^{11}Be

This PNC mixing is about one order of magnitude stronger than the scale of single-particle PNC mixing in “normal” nuclear states that can be extracted from Eq. 20. In the case of normal $p - s$ mixing, we have

$$\begin{aligned} |f_{sp}^{normal}| &= \frac{|\langle 1p|W_{sp}|2s\rangle|}{\omega} = \frac{Gg_n^W \rho_0}{\sqrt{2}m} \left(\frac{m}{\omega}\right)^{1/2} \\ &\simeq 0.7 \times 10^{-7} g_n^W \simeq 0.7 \times 10^{-7} \quad (\text{for } g_n^W \simeq 1) \end{aligned} \quad (23)$$

in the same region of nuclei with $A \sim 11$. The above value 23 for the normal PNC mixing is rather universal and it is practically insensitive to variations of the details of the normal nuclear wave functions and core densities [26]. One should stress that in the halo case, the energy denominator in Eq. 22 is $\omega/|\Delta E_{HALO}| \simeq 50$ times smaller than in the normal case 23, based on the oscillator model. Comparing Eqs. 22 and 23, we find the halo enhancement factor in the PNC mixing to be

$$\frac{|f_{sp}^{HALO}|}{|f_{sp}^{normal}|} \simeq 9.$$

This result is quite remarkable in a number of respects. First, it is seen that in experiments when the halo wave functions in nuclear exterior are probed, the value of PNC mixing is even stronger than in “normal” nuclei. Secondly, this PNC mixing is dominated by the neutron weak constant g_n^W . Such experiments with neutron halo nuclei therefore provides a unique opportunity to probe the value of this constant. Usually, the sensitivity of experiments to the value of this constant is “spoiled” by comparably large value of the proton weak constant g_p^W , cf. Eq. 7.

In order to assess the reliability of these results, one can verify the stability of the enhancement factor against variations in the parameters of the halo wave functions. As one can see from the results presented in Table 10.1, the matrix element 19 is changed by few per cent only when the wave functions are deformed. The enhancement factor 22 is therefore quite stable.

	$r_0 = 1.40$	$r_0 = 1.45$	$r_0 = 1.50$
$r_1 = 1.75$	1.168	1.052	0.950
$r_1 = 1.80$	1.110	1.000	0.903
$r_1 = 1.85$	1.056	0.952	0.860

Table 10.1 - Stability analysis for the matrix element of W_{sp} between the halo states $2s_{1/2}$ and $1p_{1/2}$. The results for the values of the parameters r_0 and r_1 differing from the best values are shown. The central entry in the table corresponds to the best value. It is seen that variations in r_0 and r_1 do not affect $\langle 2s_{1/2}|W_{sp}|1p_{1/2}\rangle$ any considerably.

The analysis presented above rests basically on the most reliably known facts: the quantum numbers of the states involved, the halo radii which match the matter radii known

from experiment, and the Hartree-Fock wave functions. With these input data, the further quantitative analysis is a straightforward analytical exercise which does not require any approximations. The stability of the results has been checked analytically. The PNC enhancement factor of one order of magnitude allows one to speak about qualitative halo effect that should not be overlooked.

It is the matter of further studies to check the universality of the effect while going along the table of exotic nuclei. One sees that other exotic nuclei with developed halo structure manifest similar properties (see, e.g., [12]). Indeed, the effect of PNC enhancement shown here results basically from the two facts:

- (i) small energy separation between the mixed opposite parity states
- (ii) considerably strong overlap between the mixed wave functions and the core density, which saves part of suppression in the PNC weak matrix element.

The first of these points is rather common for nuclei with developed neutron halos. Systematics of separation energies for single neutron [13] shows that the ground states of halo nuclei can be distanced from the continuum by typical spacing $\varepsilon_{halo} \sim (2mr_{halo})^{-1/2} \sim$ few hundreds of keV. Even in the cases when no bound states with parity opposite to that of the ground state occur, the PNC admixtures to the ground state wave functions must exist. In these cases, the PNC admixtures can be evaluated by means of Green function method.

The second point (ii) is related to the wave function structure. It would be also interesting to study the PNC effects in proton rich nuclei [20, 21, 22].

The results shown here are based on the single-particle approximation (one-body halo model). In principle, the halo neutron can couple to excitations of the core (see, e.g., Ref. [34]). In fact, such coupling can be responsible for the small energy separation between the opposite parity levels in ^{11}Be , which can be separated by few MeV otherwise (see, e.g., [23]). These many-body effects may be important for precise evaluation of the PNC mixing. We did not consider contribution from such effects here.

One of possible experimental manifestations of the discussed effect is related to anapole moment (discussed in the next Section) [24, 25] which attracts much attention in current literature [31] in view of new experimental results (detection of anapole moment in the nucleus ^{133}Cs [32]). Since the anapole moment is created by the toroidal electromagnetic currents which results from PNC, its value grows as the size of the system increased [25]. In the case of halo which we considered here, the value of the anapole moment can be therefore enhanced due to extended halo cloud. We will discuss this feature in the next Section.

0.8 Anapole moment of an exotic nucleus

The nuclear anapole moment is one of the most interesting manifestations [24, 25, 35, 29, 30, 36, 37, 31, 32] of the spatial Parity Nonconservation (PNC) [1, 2] in atomic physics. It arises from the PNC nuclear forces which create anomalous (toroidal) contributions to

the electromagnetic current. The resulting PNC magnetic field can be experienced by an external lepton (e.g., atomic electron or muon in mesic atom) and can be detected in hyperfine structure atomic measurements. The effect of the anapole moment, which depends on the nuclear spin, can be experimentally separated from other PNC contributions [37, 31, 32]. Few theoretical papers have been devoted to the problem of nuclear anapole moments [25, 35, 29, 30, 36]. The first calculation of the quantity in the single-particle approximation has been done by Flambaum and Khriplovich [25]. Calculation of the anapole moment with accounting for residual pion-mediated interaction has been made by Haxton, Henley, and Musolf [29], where an expression for the anapole moment operator has been derived, which preserves the gauge invariance automatically. In Ref. [36] various many-body corrections to the anapole moments (basically, the many-body contributions to the current) have been taken into account. This field attracts much attention [36, 37, 31, 32, 7] as some experimental results for the nuclear anapole in Cs are available [37, 32].

The studies of the anapole moment have been mostly confined to the case of normal nuclei. Specific structure of exotic nuclei [11, 12, 13, 15, 16, 20, 21, 22, 34, 38, 39, 40, 41] can offer new possibilities to probe those aspects of nuclear interactions which are not accessible with normal nuclei. The problem of the PNC effects in exotic nuclei has been addressed in the last sections [19] where it was shown that the PNC mixing in halo nuclei can be considerably enhanced as compared to the case of normal nuclei. It is therefore interesting to examine the anapole moments of the exotic nuclei.

Let us estimate the anapole moment of an exotic halo nucleus, focusing on the case of ^{11}Be which has been extensively studied both experimentally and theoretically [11, 12, 13, 15, 16]. We call the resulting anapole moment “anomalous” as it exceeds by fifteen times the average anapole moment of a normal nucleus of the same mass and is bigger than the anapole moment of any known neutron-odd nucleus. The value of the anapole moment is even twice bigger than that of lead.

Supplement B

0.9 Nuclear spin dependent PNC interaction of a lepton with nucleus via the anapole moment

The part of the Hamiltonian of the nucleus-lepton system in which we are interested in can be written in the form

$$H = H_0^n + V_{res}^n + W_{PNC}^n + H_{PNC}^{n-e} + h_{PNC}^{n-e}, \quad (24)$$

where $H_0^n = \sum_i [\mathbf{p}_i^2/2m + U_S(\mathbf{r}_i)]$ is the single particle Hamiltonian of the nucleons with momentum \mathbf{p} and mass m in the single-particle potential $U_S(r)$; V_{res}^n is the residual strong interaction.

0.9. NUCLEAR SPIN DEPENDENT PNC INTERACTION OF A LEPTON WITH
NUCLEUS VIA THE ANAPOLE MOMENT

The operator W_{PNC}^n is the weak PNC nucleon-nucleon interaction [1]. The term H_{PNC}^{n-e} describes the interaction of the lepton with the vector potential \mathbf{A}_{PNC} created by the nucleus, in which we save only the PNC part,

$$H_{PNC}^{n-e} = e(\alpha \cdot \mathbf{A}_{PNC}) = e(\alpha \cdot \langle \mathbf{a} \rangle) \Delta(\mathbf{r}) \quad (25)$$

where α denote the Dirac matrices [33] for the lepton and $\Delta(r)$ is a function sharply peaked in the region of the nucleus (it reduces to the δ -function on the scale of the atomic electron spatial motion), e is the proton charge, $e^2 = 1/137$. The last term, h_{PNC}^{n-e} , is the part of the neutral current interaction contributing to the PNC nucleus-lepton forces depending on nuclear spin,

$$h_{PNC}^{n-e} = \kappa_{nc} \frac{G}{\sqrt{2}} \frac{[1/2 - (-1)^{j+l+1/2}(j+1/2)]}{j(j+1)} (\mathbf{j} \cdot \alpha) \Delta(\mathbf{r}), \quad (26)$$

where $\kappa_{nc} \equiv (5/8)(1 - 4 \sin^2 \theta)$ with θ the Weinberg angle.

The vector $\langle \mathbf{a} \rangle$ is the expectation value of the anapole moment operator

$$\mathbf{a} = -\pi \int d^3r r^2 \mathbf{J} \quad (27)$$

in the nuclear ground state, where J is the nuclear electromagnetic current. Its is convenient to define the ‘‘anapole moment’’, κ , rewriting Eq. 25 according to [35]

$$H_{PNC}^{n-e} = e(\alpha \cdot \langle \mathbf{a} \rangle) \Delta(\mathbf{r}) \equiv \kappa \frac{G}{\sqrt{2}} \frac{(-1)^{j+l+1/2}(j+1/2)}{j(j+1)} (\mathbf{j} \cdot \alpha) \Delta(\mathbf{r}), \quad (28)$$

where j is the nuclear spin in the ground state which coincides with the angular momentum of the external nucleon if one works in the single-particle approximation; where $G = 10^{-5} m^{-2}$ is the Fermi constant and m is the nucleon mass. The factors depending on j and on the orbital angular l of the external nucleon absorb the spin-angular dependence of the anapole expectation value $\langle a \rangle$, and the anapole moment κ chosen in this way contains merely the nuclear structure information.

In the single-particle approximation, the most important part of the anapole moment operator 27 can be written [35, 29] as the sum of the spin-current term and an additional term δa

$$\mathbf{a} = \frac{\pi e}{m} \sum_i \mu_i (\mathbf{r}_i \times \sigma_i) + \delta \mathbf{a}, \quad (29)$$

which includes other contributions. Here, σ are the spin Pauli matrices, μ are the nucleon magnetic moments (+2.79 for proton and -1.91 for neutron). The last term in Eq. 29 abbreviates contribution from the orbital current and the corrections which come basically from the interaction many-body contributions (e.g., from the weak forces) to the electromagnetic current [25, 29, 36]. They are proportional to the charge of the external nucleon, and in our case (external neutron) the first term in Eq. 29 dominates in the single-particle approximation.

The expectation value of 29 in any eigenstate of the nuclear Hamiltonian, $H_0^n + V_{res}^n$ is zero unless parity violating forces W_{PNC}^n are taken into account. As a result of the PNC weak interaction W_{PNC}^n in the Hamiltonian 24, a nuclear state of definite parity $|\psi\rangle$, acquires very small admixtures of wrong parity configurations $|\bar{\psi}_n\rangle$. This can be accounted for by using the first order of perturbation theory with respect to W_{PNC}^n . Thus the expectation value of the anapole moment operator \mathbf{a} in the state $|\tilde{\psi}\rangle$ with energy E containing the PNC admixtures is

$$\langle \tilde{\psi} | \mathbf{a} | \tilde{\psi} \rangle = \sum_n \left(\frac{\langle \psi | W_{PNC} | \bar{\psi}_n \rangle}{E - E_n} \langle \bar{\psi}_n | \mathbf{a} | \psi \rangle - \langle \psi | \mathbf{a} | \bar{\psi}_n \rangle \frac{\langle \bar{\psi}_n | W_{PNC} | \psi \rangle}{E_n - E} \right) \quad (30)$$

where sum runs over the opposite parity states $|\bar{\psi}_n\rangle$. In a finite nucleus, a nucleon experiences the combined action of the two-body PNC forces W_{PNC} [1] from other nucleons, which can be modeled [2] by the effective one-body PNC weak potential w_{PNC} (see Eq. 8)

$$w_{PNC} = g \frac{G}{2\sqrt{2}m} \{(\boldsymbol{\sigma} \cdot \mathbf{p}), \rho\},$$

where the curly brackets denote anticommutator. The nuclear core density $\rho = \sum_{occ} |\psi_{occ}|^2$ in 6 reflects the coherent contribution from all the occupied nucleon orbitals. The dimensionless constants g for proton and neutron are $g_p = 4.5 \pm 2$, $g_n = 1 \pm 1.5$. These widely used values [2, 25, 35, 26] correspond to the best values [1] of the microscopic parameters in the DDH Hamiltonian [1]. They are found in reasonable agreement with the bulk experimental data on PNC including the compound nuclear experiments by TRIPLE group [3] and anapole moments of stable nuclei [32].

0.10 Weak interaction and the anapole moment in halo nucleus

The basic specific properties of the halo nuclei are determined by the fact of existence of loosely bound nucleon in addition to the core composed by the rest of the nucleons [13].

In one-body halo nuclei like ^{11}Be , the ground state is particularly simple: it can be represented as direct product of the single-particle wave function of the external neutron, ψ_{halo} , and the wave function of the core. The spin-saturated core does not contribute to 30. The residual interaction V_{res}^n in Eq. 24 can be neglected as the many-body effects related to the core excitations are generically weak in such nuclei [34]. As a result of the relatively heavy core for $A \simeq 10$, difference between the center of mass coordinate and the center of core coordinate can also be neglected. The problem with the Hamiltonian 24 and 6 is reduced to a single-particle problem for the external nucleon. For the nucleus with the external *neutron*,

as is the case for the halo nucleus ^{11}Be , the orbital part of the anapole operator 29 does not contribute. Using the reduced matrix elements of the spin-angular part of the operator 29,

$$\langle l', j, m | \frac{\mathbf{r}}{r} \times \sigma | l, j, m \rangle = i(-1)^{j+l+1/2}(j+1/2) \sqrt{\frac{2j+1}{j(j+1)}}, \quad l' = l \pm 1,$$

the anapole moment can be expressed in terms of the radial wave functions R_{nlj} as follows:

$$\begin{aligned} \kappa = & -\frac{2\pi\mu_n e^2 g_n}{m^2} \sum_{n'l'j} \int_0^\infty r^2 dr R_{n'l'j} [\rho (dR_{nlj}/dr + (l-j)(2l+1-j)R_{nlj}/r) \\ & + (d\rho/2dr) R_{nlj}] \int_0^\infty r^3 dr R_{n'l'j} R_{nlj} / (E_{nlj} - E_{n'l'j}). \end{aligned} \quad (31)$$

In a halo nucleus like ^{11}Be or ^{11}Li , the energy spacing between the opposite parity weakly-bound states can be small [11, 12, 13, 15, 16, 34]. The PNC effect in 31 can therefore be considerably magnified [19]. The nucleus ^{11}Be has the only bound excited state, $1p_{1/2}$, above the ground state $2s_{1/2}$ [11, 12, 15, 16] (inversion of levels). As a result of the small energy separation between these levels of opposite parities which is known experimentally, Eq. 21, one can save the only $1p_{1/2}$ term in the expression 31 for the anapole moment κ of the ground state $2s_{1/2}$. The form of the single-particle wave functions of halo states can be deduced from their basic properties [16] and their quantum numbers [12]. The results of the Hartree-Fock calculations which reproduce the main halo properties (e.g., mean square radii) are also available [12]. We use the following ansatz [19, 9] for the model wave functions of the $2s$ and the excited $1p$ halo states as given by Eq. 10. The core nucleon density $\rho_c(r)$ has been taken according to Eq. 15, as shown on Fig. 4(a). Evaluation of Eq. 31 with the wave functions 10 and the core density 15 gives the expression for the anapole moment in terms of the parameters of Eq. 16.

The results for the densities are shown in Fig.4(a). One sees good agreement with the Hartree-Fock calculations [12]. The values of the halo radii given by 13, $\sqrt{\langle r_{2s}^2 \rangle} = 5.9$ fm and $\sqrt{\langle r_{1p}^2 \rangle} = 4.9$ fm are close to the values of Ref.[12] 6.5 fm and 5.9 fm which agree with experimental matter radii.

With the above values of the parameters, one obtains from 31 the resulting value of the anapole moment κ

$$\kappa (^{11}\text{Be}) = 0.17g_n = 0.17 \quad (\text{for } g_n \simeq 1). \quad (32)$$

It is few times bigger than the contribution from neutral current $-\kappa_{nc} = -0.05$. Thus the nuclear spin-dependent PNC interaction of a lepton with the halo nucleus is dominated by the anapole moment contribution, as in heavy nuclei.

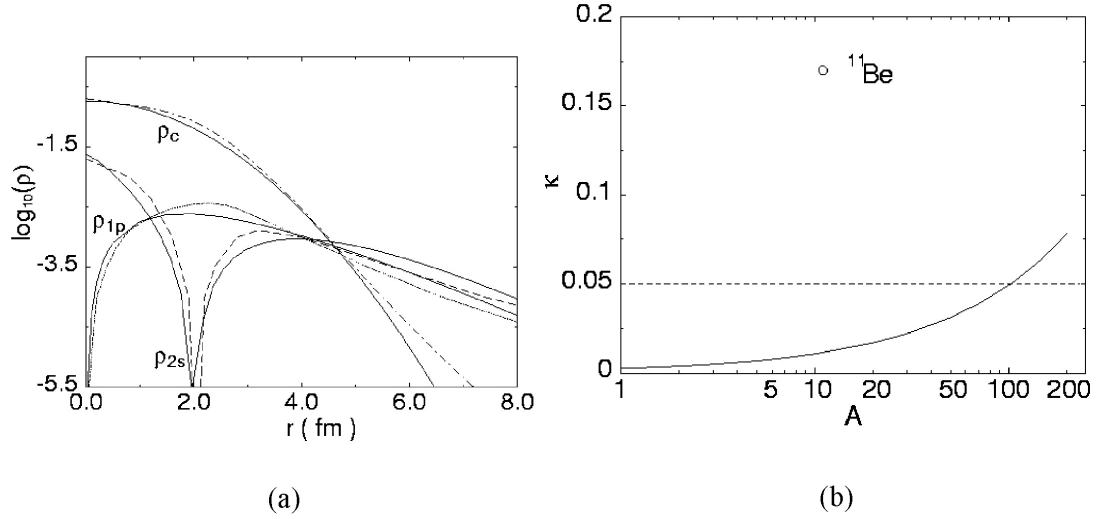


Figure 4: (a) Densities $R^2(r)$ for the halo states $2s$ and $1p$ as function of r and the core density $\rho_c(r)$ calculated from Eqs. (10,15) (solid lines). The Hartree-Fock results for the same quantities [12] are given by the dashed line, the dotted line and the dotted-dashed line, respectively. (b) “Halo anomaly” in ^{11}Be : the value $\kappa(^{11}\text{Be})$ (circle) as compared to the absolute values of the anapole moments of normal neutron-odd nuclei (solid curve) and the neutral current contribution $\kappa_{nc} = 0.05$ (dashed curve).

To appreciate how big the value $\kappa(^{11}\text{Be})$ is, one can compare 32 to the anapole moment of the normal spherical nucleus with odd neutron which is given by [35]:

$$\kappa_{norm} = \frac{9}{10} \frac{g_n e^2 \mu_n}{m r_0} A^{2/3}, \quad (33)$$

where $r_0 = 1.2$ fm is the nucleon radius. Resulting from the PNC toroidal electromagnetic currents, the anapole moment grows fast ($\propto A^{2/3}$) as the size of the system increases [25, 35]. For this reason, the anapole moments of *normal* light nuclei give only a small correction to the neutral current lepton-nucleus PNC interaction (see Fig. 4(b)). From 32 and 33, we find the ratio of the anapole moment to its value in a nucleus with the same A (enhancement factor):

$$R_{halo} = \frac{\kappa(^{11}\text{Be})}{\kappa_{norm}} = 15. \quad (34)$$

In fact, the anapole moment 32 exceeds few times the anapole moments of any known odd nucleus, as seen in Fig.4(a). For example, the $\kappa(^{11}\text{Be})$ is two times bigger than the anapole moment of nucleus as heavy as lead [35],

$$\kappa(^{207}\text{Pb}) = -0.08g_n.$$

The remarkable enhancement factor 34 in 32 comes from the two features of the halo structure: a) enhancement of the PNC mixing in the halo ground state [the first factor in Eq. 35] and b) enhancement of the matrix elements of the anapole operator in halo states:

$$R_{halo} \sim \frac{\omega}{\Delta E} \left(\frac{w_{halo}}{w_{norm}} \right) \left(\frac{r_{halo}}{r_{norm}} \right), \quad (35)$$

where the second factor is the ratio of the halo weak matrix element w_{halo} , Eq. 6, to the normal one, w_{norm} , which is less than unity. The parity violating effect originates from the weak interaction of the external halo neutron with the core nucleons in the nuclear interior. As a result, the neutron halo cloud surrounding the nucleus acquires the wrong parity admixtures. Those give rise to the PNC toroidal currents in the nuclear exterior (the halo region) which results in additional enhancement of the anapole moment [the last factor in 35].

0.11 Many-body corrections to the anapole moment

We discuss now the stability of the results against possible distortions of the wave functions 10. Table 10.2 shows the values of the anapole moment calculated for various values of the parameters r_0 and r_1 in the wave functions 10. As is seen from the Table, the results are stable with respect to variation of the details of the halo structure.

	$r_0 = 1.35$	$r_0 = 1.40$	$r_0 = 1.45$	$r_0 = 1.50$	$r_0 = 1.55$
$r_1 = 1.70$	1.26	1.15	1.05	0.96	0.87
$r_1 = 1.75$	1.23	1.12	1.03	0.94	0.85
$r_1 = 1.80$	1.19	1.09	1.00	0.91	0.83
$r_1 = 1.85$	1.16	1.06	0.97	0.89	0.81
$r_1 = 1.90$	1.12	1.03	0.95	0.87	0.80

Table 10.2 - Dependence of $\kappa(^{11}Be)$ on the halo parameters r_0 and r_1 in Eq.16; the ratios of κ to the result 19 are given. The central entry in the table corresponds to the optimal values used in 19. It is seen that variations in r_0 and r_1 do not appreciably affect 19.

We consider now the influence of possible many-body contributions (see, e.g., [39, 40]) to the halo wave functions 10 on the present results based on single-particle picture.

The generalized wave function of the halo ground state, $|s\rangle$, can be written as a sum

$$|s\rangle = (1 - x_s^2)|s_{sp}\rangle + x_s|S_{mb}\rangle,$$

where $|s_{sp}\rangle$ is the purely single-particle s-state in Eqs. 30 and 10, and $|S_{mb}\rangle$ denotes the many-body contributions due to core polarization, deformations *etc.*, which have not been

considered yet. The coefficient x_s ($0 \leq x_s \leq 1$) is the amplitude of the many-body contribution which is assumed to be properly normalized, $\langle S_{mb}|S_{mb}\rangle = 1$. The anapole moment can be evaluated in the same way as above, using Eqs. 29, 30 and 6 and substituting the state $|s\rangle$ instead of $|s_{sp}\rangle$. Both the anapole moment operator 29, the weak potential 6 are the single-particle operators, so they can not connect the single-particle wave function $|p_{sp}\rangle$ 10 with the many-body component $|S_{mb}\rangle$. Thus

$$\langle S_{mb}|\mathbf{a}|p_{sp}\rangle = 0 \quad \text{and} \quad \langle S_{mb}|w_{PNC}|p_{sp}\rangle = 0. \quad (36)$$

The anapole moment $\tilde{\kappa}$ in the state $|s\rangle$ is now given by the simple renormalization of the result obtained above,

$$\tilde{\kappa} = (1 - x_s^2)\kappa,$$

where κ is the single-particle result 31, 16 and 32. Similarly to Eq. 36, one can take into account many-body contributions $|P_{mb}\rangle$ to the excited p-state $|p_{sp}\rangle$ (10) with the amplitude x_p , $|p\rangle = (1 - x_p^2)|p_{sp}\rangle + x_p|P_{mb}\rangle$. In this case, the modified result for the anapole moment is:

$$\tilde{\kappa} = \kappa \left[(1 - x_s^2)(1 - x_p^2) + x_s x_p \sqrt{(1 - x_s^2)(1 - x_p^2)}(u + v) + x_s x_p uv \right], \quad (37)$$

where $u = \langle S_{mb}|\mathbf{a}|P_{mb}\rangle / \langle s_{mb}|\mathbf{a}|p_{mb}\rangle$ and $v = \langle S_{mb}|w_{PNC}|P_{mb}\rangle / \langle s_{mb}|w_{PNC}|p_{mb}\rangle$ denote the ratios of the matrix elements of the anapole (weak interaction) between the many-body components S_{mb} and P_{mb} to their values for the single-particle states. One can note that the matrix elements of the single-particle operators between the many-body wave functions are generically suppressed as compared to those between the single-particle states, so that the factors u and v can be neglected for the sake of estimate.

According to experimental results [41], the many-body contributions to the halo ground state in ^{11}Be are rather small, $\approx 16\%$. Assuming the many-body corrections to the excited states of the same magnitude, $x_p \simeq x_s$, one can conclude from Eq. 37 that the results obtained in the single-particle approximation could hardly be reduced by more than 30 per cent.

The corrections due to the many-body admixtures in the halo states are therefore about the same order of magnitude as the many-body corrections to the operators 29 and 6. They can be taken into account in more refined calculations using detailed information on the wave function structure.

The curious ‘‘halo anomaly’’ illustrated in Fig. 4(b) can be quite interesting in a number of respects. First, the search for sources of enhancement in anapole moments has been always important from the experimental viewpoint. Possibilities offered by the normal nuclei are rather limited here. The most promising case of deformed nuclei, where one can find close levels of opposite parity near the ground state, does not offer any enhancement because of the suppression in the matrix elements of \mathbf{a} [35]. In this respect, the anomalies in anapole moments of exotic nuclei like ^{11}Be seem to give unexpected opportunity. Secondly, the

anapole moment of neutron-rich nuclei is determined by the neutron weak constant g_n only. Usually, the sensitivity of experiments to the value of this constant is “spoiled” by relatively large value of the proton weak constant g_p , in Eq.6. The large enhancement of the anapole moment in neutron halo nuclei provides therefore an unique opportunity to test the isospin structure of the weak potential δ which is of great interest [7].

One should note that the nucleus ^{11}Be has a rather long life-time (13.81 sec). This makes therefore possible, at least in principle, the atomic measurements of the hyperfine structure effects in traps planned for the ISOL facility where the anapole moment can be detected.

It would be also interesting to consider mesic atoms with exotic nuclei, where the effect can be further enhanced, as the heavy lepton orbits are closer to nucleus than in usual atoms. The case of proton rich nuclei where the effect must be more pronounced due to numerical value of the constant g_p , is also of separate interest.

0.11. MANY-BODY CORRECTIONS TO THE ANAPOLE MOMENT

Bibliography

- [1] B. Desplanques, J. Donoghue, and B. Holstein, *Ann. Phys. (N.Y.)* **124** (1980) 449
- [2] E.G. Adelberger and W.C. Haxton, *Ann. Rev. Nucl. Part. Sci.* **35** (1985) 501.
- [3] J.D. Bowman, C.D. Bowman, J.E. Bush, P.P.J. Delheij, C.M. Frankle, C.R. Gould, D.G. Haase, J. Knudson, G.E. Mitchel, S. Penttila, H. Postma, N.R. Robertson, S.J. Seestrom, J.J. Szymansky, V.W. Yuan, and X. Zhu, *Phys.Rev.Lett.* **65** (1990) 1192.
- [4] M.B. Johnson, J.D. Bowman, and S.H.Yoo, *Phys. Rev. Lett.* **67** (1991) 310.
- [5] O.P. Sushkov and V.B. Telitsin, *Phys. Rev.* **C48** (1993) 1069.
- [6] B. Desplanques, *Phys. Rep.* **297** (1998) 1.
- [7] W.S. Wilburn and J.D. Bowman, *Phys. Rev.* **C57** (1998) 3425.
- [8] D.B. Kaplan, M.J. Savage, R.P. Springer, and M.B. Wise, *Phys. Lett.* **B449** (1999) 1.
- [9] H. Feshbach, M.S. Hussein, A.K. Kerman, and O.K.Vorov, *Adv. Nucl. Phys.* **25**
- [10] J.S. Al-Khalili and J.A. Tostevin, *Phys. Rev. Lett.* **76** (1996) 3903.
- [11] R.C. Johnson, J.S. Al-Khalili, and J.A. Tostevin, *Phys. Rev. Lett.* **79** (1997) 2771.
- [12] H. Sagawa, *Phys. Lett.* **B286** (1992) 7.
- [13] C.A. Bertulani, L.F. Canto, and M.S. Hussein, *Phys. Rep.* **226** (1993) 281.
- [14] C.A. Bertulani, L.F. Canto, and M.S. Hussein, *Phys. Lett.* **B353** (1995) 413.
- [15] K. Hencken, G. Bertsch and H. Esbensen *Phys. Rev* **C54** (1996) 3043.
- [16] A. Mengoni, T. Otsuka, T. Nakamura, and M. Ishihara, Contribution to the 4th International Seminar on Interaction of Neutrons with Nuclei, Dubna (Russia), April 1996, Preprint nucl-th/9607023.

- [17] J. Hardy, In *Physics of Unstable Nuclear Beams*, C.A.Bertulani, L.F.Canto, and M.S.Hussein ed., World Scientific, Singapore, 1997.
- [18] T. Suzuki, In *Physics of Unstable Nuclear Beams*, C.A.Bertulani, L.F.Canto, and M.S.Hussein ed., World Scientific, Singapore, 1997, p.157.
- [19] M.S. Hussein, A.F.R. de Toledo Piza, O.K. Vorov, and A.K. Kerman, Phys. Rev. **C60**, (1999), 064615.
- [20] B.A. Brown and P.G. Hansen, Phys. Lett. **381B** (1996) 391.
- [21] S. Karataglidis and C. Bennhold, Phys. Rev. Lett. **80** (1998) 1614.
- [22] Z.Z. Ren, A. Faessler, and A. Bobyk, Phys. Rev. **C57** (1998) 2752.
- [23] H. Sagawa and K. Yazaki, Phys. Lett. **B244** (1990) 149.
- [24] Ya.B. Zel'dovich, Zh.Exp.Teor.Fiz. **33** (1957) 1531 [Sov. Phys. JETP **6** (1957) 1184].
- [25] V.V. Flambaum and I.B. Khriplovich, Zh. Eksp. Teor. Fiz. **79** (1980) 1656 [Sov.Phys. JETP **52** (1980) 835]; V.V. Flambaum and I.B. Khriplovich and O.P. Sushkov, Phys. Lett. **B146** (1984) 367.
- [26] V.F. Flambaum and O.K. Vorov, Phys. Rev. Lett. **70** (1993) 4051.
- [27] V.F. Flambaum and O.K. Vorov, Phys. Rev. **C51** (1995) 1521.
- [28] N. Auerbach and B.A. Brown, Phys. Lett. **B340** (1994) 6.
- [29] W.C. Haxton, E.M. Henley, and M.J. Musolf, Phys. Rev. Lett. **63**, 949(1989).
- [30] C. Bouchiat and C.A. Piketty, Z. Phys. **C49** (1991) 91.
- [31] W.C. Haxton, Science, **275** (1997) 1753.
- [32] C.S. Wood, S.C. Bennet, D. Cho, B.P. Masterson, J.L. Roberts, C.E. Tanner, and C.E. Wieman, Science **275** (1997) 1759.
- [33] A. Bohr and B. Mottelson, *Nuclear Structure* (Benjamin, New York, 1969), Vol. 1.
- [34] T.T.S. Kuo, F. Krmpotic, and Y. Tzeng, Phys. Rev. Lett. **78** (1997) 2708.
- [35] V.V. Flambaum, I.B. Khriplovich, and O.P. Sushkov, Phys.Lett. **146B**, (1984), 367 , Preprint INP-84-89; Phys. Lett. **B162**, (1985), 213; Nucl. Phys. **A449**, (1986), 750.
- [36] V.F. Dmitriev, I.B.Khriplovich and V.B. Telitsin, Nucl. Phys. **A577**, (1994), 691.

-
- [37] M.S. Noecker, B.P. Masterson and C.E. Wieman, Phys. Rev. Lett. **61**, (1988), 310.
- [38] W. Nazarewicz, J. Dobaczewski, and T.R. Werner, Phys. Scr. **T56**, (1995), 9.
- [39] D.J. Millener, J.W. Olness, E.K. Warburton, and S.S. Hanna, Phys. Rev. **C28**, (1983), 497.
- [40] F.M. Nunes, I.J. Thompson, and R.C. Johnson, Nucl. Phys. **A596**, (1996), 171; N.K. Timofeyuk and R.C. Johnson, Phys. Rev. **C59**, (1999), 1545.
- [41] S. Fortier et. al., Phys. Lett. **B461**, (1999), 22.